USING SENTAURUS MOnte CArlo(MOCA) SIMULATION ESTIMATION OF SCATTERING EFFECTS IN NANOWIRE TRANSISTORS

Mr.S.Esakki Rajavel[1], A.GunaDhivya Vinisha[2], J.Jochebed[3],P.Angelene Sanjana[4], D.Gnancy[5]

Abstract-The control of short – channel effects is more challenging with the progressive scaling of metal -oxide-semiconductor field –effect-transistors (MOSFETs).The double –gate (DG) and gate –all –around (GAA) MOSFET structures have emerged as main candidates to provide the electrostatic integrity needed to scale down MOSFET to minimal channel lengths. In addition to a better electrostatics than the single – gate (SG) MOSFET, the use of these devices as advantages relative to the carrier transport, mainly due to Sentaurus MOCA(MOnte CArlo) using monte carlo simulation. More-over the introduction of new materials to enhance the mobility, as the strained silicon can result in electronic transport approaching the ballistic regime. The international roadmap for semiconductors (ITRS-200) has identified a series of challenges that must be solved before these devices can enter the manufacturing of MOSFET-based integrated circuits.

Keywords— Sentaurus MOCA; monte carlo simulation; electrostatic integrity

I INTRODUCTION

RECENTLY, The nanowire transistor has begun to attract a great deal of attention. If the downsizing of the conventional device ever promotes the quasi- or near-ballistic transport of carriers, the potential for performance improvement by further downscaling seems unpromising or, rather, the resultant shorter channel length may lead to the degradation of the off current.

[1] Assistant Professor/ECE, Francis Xavier Engineering College, Tirunelveli

[2] U.G.Scholar/ECE, Francis Xavier Engineering College, Tirunelveli

[3] U.G.Scholar/ECE, Francis Xavier Engineering College, Tirunelveli

[4] U.G.Scholar/ECE, Francis Xavier Engineering College, Tirunelveli

[5] U.G.Scholar/ECE, Francis Xavier Engineering College, Tirunelveli

As a limiting structure of the advanced Fin-FET approach, the nanowire FET, where a small number of conducting channels within the device can be closely controlled by the gate electrode, may be promising as a next generation device structure. In particular, the carbon nanotube FET seems advantageous due to its large carrier velocity and the smooth channel surface that release from the interface scattering. On the other hand, the advantage for silicon nanowire MOSFET lies in the availability of the many silicon technologies that have accumulated so far.

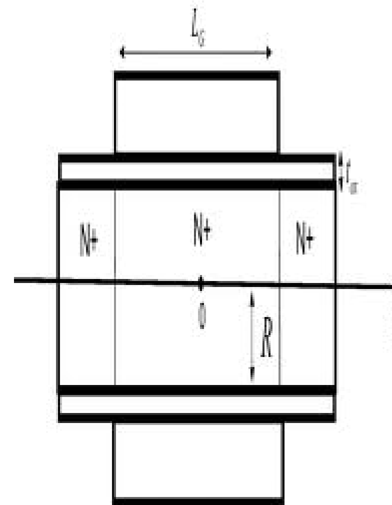

Fig1: Schematic cross-section of the Si NW

II.MATERIALS AND METHODS

A.SENTAURUS MOCA

The Sentaurus Device Monte Carlo consists of two modules for Monte Carlo simulations – Sentaurus MOCA and Sentaurus SPARTA – as well as the band-structure calculator Sentaurus Band Structure.Sentaurus MOCA (MOnte CArlo) and Sentaurus SPARTA (Single-PARTicle Approach) are self-consistent, full-band Monte Carlo simulators useful for the analysis of submicron

 All Rights Reserved © 2014 IJARCET

devices. Both tools allow quasi-ballistic and hot-electron effects to be taken into account.

These are important for the accurate determination of terminal currents. In addition, internal variables, such as carrier density and carrier velocity, are computed and saved for visualization. In Sentaurus MOCA, an ensemble of particles (electrons or holes) is distributed in the device, and particles are injected and removed from contacts during the simulation. All particles are propagated in the device using the instantaneous electric field obtained by solving the Poisson equation for a short synchronous time step and, if selected, the Schrödinger equation. The procedure is iterated for a specified simulation time. Since the ensemble of particles can model the real transient behavior of the charge carriers, Sentaurus MOCA can be used to model both transient and steady-state behavior.

Sentaurus MOCA can also be used to study the effect of plasma oscillations on electronic transport. This is important for capturing saturation-current degradation for gate lengths less than 40 nm

Sentaurus MOCA contains two simulators in one tool:

■ **A bulk (zero-dimensional) simulator** for fitting material parameters to experimental data.
This is the classic unipolar, space-homogeneous research code that can be used to
investigate femtosecond transients or impact-ionization coefficients. This mode is
intrinsically unipolar, that is, only electrons *or* holes can be simulated.

■ **A two-dimensional device simulator, with regions of different materials**, Ohmic and
blocking contacts, quantization effects, and so on. A complete nonlinear Poisson solver is
also included. This code only shares the core subroutines (band-structure interpolation,
scattering rates, and so on) with the bulk code.

Sentaurus MOCA is designed to simulate devices that are in a high-bias condition and in
situations where very high fields are present in the device, or very fast transients. Some
situations where users should consider Sentaurus MOCA as the tool of choice include:

- MOSFETs with very short gate lengths:

• Velocity overshoot

• Accurate substrate current prediction because of excellent prediction of impact ionization

- Flash charging:

• Accurate prediction of the energy of the carrier and, therefore, tunneling or thermionic
Emission into nanocrystals or other charging materials

- ■ Bipolar with very short base or emitter length
- ■ Prediction of extremely short transient effects
- ■ Study of noise properties of a device
- ■ Prediction of transport variables for use in Sentaurus Device

B. DEVICE STRUCTURE AND SIMULATION

The international roadmap for semiconductors (ITRS-200) has identified a series of challenges that must be solved before these devices can enter the manufacturing of MOSFET-based integrated circuits.

The scattering rates used in Sentaurus MOCA are based on the energy-dependent models
Both inelastic acoustic phonon modes and optical phonon modes are included to produce physical drift velocity versus field results.

The derivation for the phonon scattering rates below is taken from the literature. The
deformation potential method follows as:

$$H' = \varepsilon \frac{dy}{dr} \tag{1}$$

Finally, Fermi's golden rule can be applied to obtain final transition probabilities that can be
applied to all scattering mechanisms

$$P(k,k') = \frac{\pi}{\rho V \omega_q} \begin{bmatrix} N_q \\ N_q + 1 \end{bmatrix} G \left| E_{ij} q_j \xi_i \right|^2 \delta[\varepsilon(k') - \varepsilon(k) \mp \hbar\omega_q] \tag{2}$$

For a non degenerate band at the center of the Brillouin zone, the deformation potential, , is
diagonal and can therefore be treated as a scalar. In this simple situation, energy and momentum conservation imply:

$$q = \mp 2\left(k\cos\theta - \frac{m^* u_l}{\hbar}\right) \tag{3}$$

One important observation to make is that when collisions are assumed to be elastic.

In general, this assumption is false and cannot

 All Rights Reserved © 2014 IJARCET

be used in Monte Carlo simulations. Keeping the same isotropic approximation for deformation potential coupling and using the Herring–Vogt transformation on k and q vectors, the magnitude of q becomes:

$$q = q^*\left[\frac{m_l}{m_0}\cos^2\theta^* + \frac{m_t}{m_0}\sin^2\theta^*\right]$$

$$q \approx \left[\frac{m_d}{m_0}\right]^{1/2} \quad (4)$$

where θ* is the angle between k* and the principal axis of the valley. This approximation is sufficient for silicon.

Electron transitions between states in two different equivalent valleys can be induced by both acoustic and optical phonons.

The phonon wave vector q involved in the transition remains close to the distance between initial and final minima, even for high electron energies. So the changes in momentum and frequencies are approximately constant and, therefore, this Scattering mechanism is treated in the same way as intravalley scattering by optical phonons.

The integrated scattering probability for intervalley scattering is then:

$$P_i(\varepsilon) = \frac{(D_iK)^2 m^{3/2} Z_f}{\sqrt{2}\pi\rho\hbar^3\omega_i}\begin{pmatrix} N_i \\ N_i+1 \end{pmatrix}(\varepsilon \pm \hbar\omega_i - \Delta\varepsilon_{fi})^{1/2} \quad (5)$$

For the mobility of carriers in the inversion layer of MOSFET devices, surface roughness

scattering is taken into account as a function of the surface normal effective field . The auto covariance of the surface roughness is modeled as either a Gaussian function or an exponential function. In Sentaurus MOCA, the latter is used, as shown here:

$$\delta(r) = \Delta^2 \cdot \exp\left(-\frac{r}{L}\right) \quad \textbf{(6)}$$

in which Δ is the root-mean-square (RMS) height of the amplitude of the roughness, and L is the correlation length.

For electrons moving in the (100) plane, the effective mass is assumed to be an average of the 2D mass of the four longitudinal ellipsoids and the 2D mass of the two transverse ellipsoids:

$$m_d = \frac{m_0}{3}\cdot[2(m_l m_t)^{1/2} + m_t] \quad (7)$$

With the introduction of an effective mass of the 2D density-of-state, the surface roughness scattering rate becomes:

$$P_{sr}(k_{//}) = \frac{m_d(eE_{eff}\Delta L)^2}{2(\hbar)^3}\int_0^{2\pi}\frac{1-\cos\theta}{[1+L^2k_{//}^2(1-\cos\theta)]}d\theta = \frac{\pi m_d(eE_{eff}\Delta)^2}{(\hbar)^3 k_{//}^2}\left[1-\frac{1}{\sqrt{1+2L^2k_{//}^2}}\right] \quad (8)$$

If the surface of the channel is oriented to a direction other than (100) by the parameter ydir the 2D effective mass of electrons changes accordingly. In addition, when a stress of considerable strength is applied to a device, the band structure of the stressed material changes, which results in a change of the effective mass. The change of the effective mass due to the surface orientation and the stress effect is taken into account automatically.

III SCATTERING

Scattering is a general physical process where some forms of radiation, such as light, sound, or moving particles, are forced to deviate from a straight trajectory by one or more localized non-uniformities in the medium through which they pass. In conventional use, this also includes deviation of reflected radiation from the angle predicted by the law of reflection. Reflections that undergo scattering are often called diffuse reflections and unscattered reflections are called specular (mirror-like) reflections.

A.RAMAN SCATTERING

Raman scattering can occur with a change in vibrational, rotational or electronic energy of a molecule (see energy level). Chemists are concerned primarily with the vibrational Raman effect.There are two types of Raman scattering, Stokes scattering and anti-Stokes scattering.

A Raman transition from one state to another, and therefore a Raman shift, can be activated optically

 All Rights Reserved © 2014 IJARCET

only in the presence of non-zero polarizability derivative with respect to the normal coordinate (that is, the vibration or rotation):

$$\left|\frac{\partial \alpha}{\partial Q}\right| > 0 \qquad (9)$$

Raman-active vibrations/rotations can be identified by using almost any textbook that treats quantum mechanics or group theory for chemistry. Then, Raman-active modes can be found for molecules or crystals that show symmetry by using the appropriate character table for that symmetry group.

B.RAYLEIGH SCATTERING

Rayleigh scattering is the elastic scattering of light or other electromagnetic radiation by particles much smaller than the wavelength of the light, which may be individual atoms or molecules. It can occur when light travels through transparent solids and liquids, but is most prominently seen in gases..Small size parameter approximation

The size of a scattering particle is parametrized by the ratio x of its characteristic dimension r and wavelength λ:

$$x = \frac{2\pi r}{\lambda}. \qquad (11)$$

Rayleigh scattering can be defined as scattering in the small size parameter regime x ≪ 1. The intensity I of light scattered by a single small particle from a beam of unpolarized light of wavelength λ and intensity I_0 is given by:

$$I = I_0 \frac{1+\cos^2\theta}{2R^2}\left(\frac{2\pi}{\lambda}\right)^4\left(\frac{n^2-1}{n^2+2}\right)^2\left(\frac{d}{2}\right)^6 \qquad (12)$$

where R is the distance to the particle, θ is the scattering angle, n is the refractive index of the particle, and d is the diameter of the particle.

$$\sigma_s = \frac{2\pi^5}{3}\frac{d^6}{\lambda^4}\left(\frac{n^2-1}{n^2+2}\right)^2 \qquad (13)$$

C.IMPURITY SCATTERING

The scattering by ionized impurities represents an elastic process. The most popular models for this type of scattering are due to Brooks and Herring and Conwell and Weisskopf. The difference between the two approaches lies in the treatment of the screening effect. In this work we adopt the Brooks-Herring model with some refinements described below.

Brooks-Herring Model

Within this model the scattering potential is given by

$$V(r) = \frac{Ze^2}{4\pi\varepsilon r}\exp(-\beta r), \qquad (14)$$

where β^{-1} is the screening length and Z denotes the number of charge units of the impurity.

Using Fermi's golden rule together with the nonparabolic band structure one obtains for the total scattering rate:

$$\lambda_{BH}(\epsilon) = \frac{\sqrt{2}N_I Z^2 e^4}{\varepsilon^2\sqrt{m_d^*\epsilon_\beta}}\sqrt{\epsilon(1+\alpha\epsilon)}\frac{1+2\alpha\epsilon}{1+4\frac{\epsilon(1+\alpha\epsilon)}{\epsilon_\beta}}, \qquad (15)$$

where parameter ϵ_β is defined by

$$\epsilon_\beta = \frac{\hbar^2\beta^2}{2m_d^*}. \qquad (16)$$

IV SIMULATION RESULTS

Sentaurus Device performs the device simulations. The set of transport models used for all simulations is:

- Drift-diffusion transport model
- Philips unified mobility model
- High-field mobility degradation
- Lucent mobility model (mobility degradation at the silicon–oxide interface)
- Density gradient quantum corrections

 All Rights Reserved © 2014 IJARCET

The following graph shows the drain current against gate voltage characteristics for the device. Two different drain biases are simulated in this project: 0.05 V and 1.0 V.

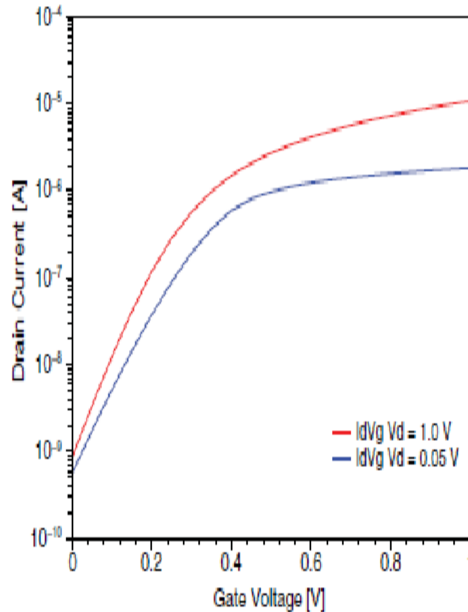

Fig2:Plot of Id–Vds characteristics

The figure 2 shows the the plot between the Id and Vds characteristics at Vd = 0.05 V (blue) and Vd = 1.0 V (red)

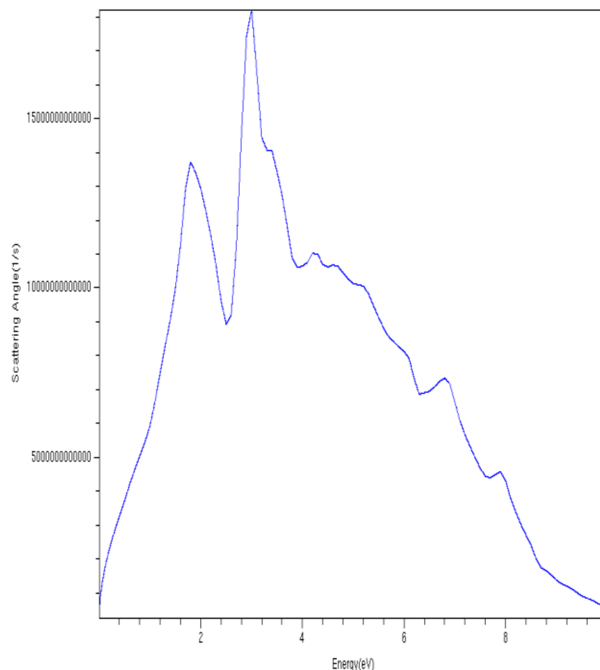

Fig3: scattering angle vs energy

The Figure 3 shows the scattering angle against energy characterstics for the device.

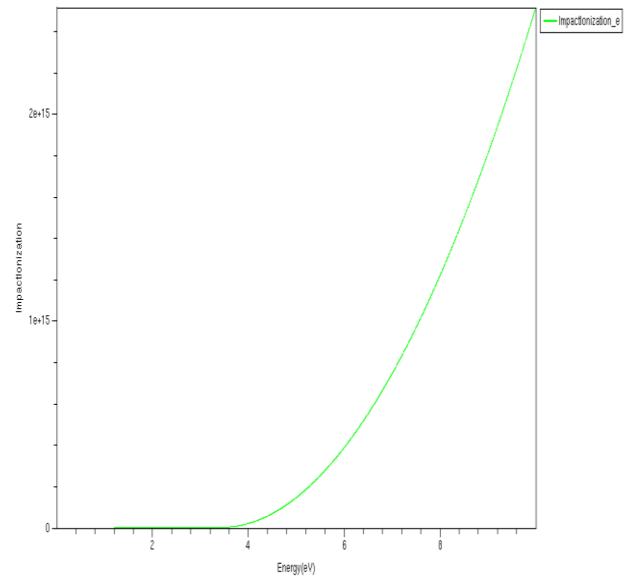

Fig 4:plot for impact ionization vs energy

The Figure 3 shows the impact ionization against energy characterstics for the device

V CONCLUSION

In this paper, the scattering effects of SILICON NANOWIRE TRANSISTOR have been described. A Monte carlo technique for the structure is presented based on surface potential formalism for different scattering types. we have clearly analyzed the parameters and characterstics of SILICON NANOWIRE TRANSISTOR

VI REFERENCES

[1] K. Natori, Y. Kimura, and T. Shimizu, “Characteristics of a carbon nanotube field-effect transistor analyzed as a ballistic nanowire fieldeffect transistor,” J. Appl. Phys., vol. 97, no. 3, pp. 034 306-1–034 306-7,Jan. 2010.

[2] D. Jimènez, J. J. Sáenz, B. Iniquez, J. Suné, L. F. Marsal, and J. Parllarès, “Unified compact model for the ballistic quantum wire and quantum well metal–oxide–semiconductor field-effect-transistor,” J. Appl. Phys., vol. 94, no. 2, pp. 1061–1068, Jul. 2008.

[3] J. Wang, A. Rahman, A. Ghosh, G. Klimeck, and M. Lundstrom, “On the validity of the parabolic effective-mass approximation for the I–V calculation of silicon nanowire transistors,” IEEE Trans. Electron Devices, vol. 52, no. 7, pp. 1589–1595, Jul. 2006.

 All Rights Reserved © 2014 IJARCET

[4] M. Lundstrom and J. Guo, Nanoscale Transistors: Device Physics, Modeling and Simulation. New York: Springer-Verlag, 2006, ch. 5.
[5] B. C. Paul, R. Tu, S. Fujita, M. Okajima, T. H. Lee, and Y. Nishi, "An analytical compact circuit model for nanowire FET," *IEEE Trans. Electron Devices*, vol. 54, no. 7, pp. 1637–1644, Jul. 2011.
[6] A. Godoy, F. Ruiz, C. Sampedro, F. Gámiz, and U. Ravaioli, "Calculation of the phonon-limited mobility in silicon gate-all-around MOSFETs," *Solid State Electron.*, vol. 51, no. 9, pp. 1211–1215, Sep. 2007.
[7] S. Jin, M. V. Fischetti, and T-W. Tang, "Modeling of electron mobility in gated silicon nanowires at room temperature: Surface roughness scattering, dielectric screening, and band nonparabolicity," *J. Appl. Phys.*,vol. 102, no. 8, p. 083 715-1, Oct. 2007.
[8] E. Gnani, A. Gnudi, S. Reggiani, M. Rudan, and G. Baccarani, "Band structure effects on the current–voltage characteristics of SNW-FETs," in *IEDM Tech. Dig.*, 2007, pp. 737–740.
[9] A. Pecchia, L. Salamandra, L. Latessa, B. Aradi, T. Frauenheim, and A. D. Carlo, "Atomistic modeling of gate-all-around Si-nanowire fieldeffect transistors," *IEEE Trans. Electron Devices*, vol. 54, no. 12,pp. 3159–3167, Dec. 2010.
[10] H. Sakaki, "Scattering suppression and high-mobility effect of sizequantized electrons in ultrafine semiconductor wire structures," *Jpn. J. Appl. Phys.*, vol. 19, no. 12, pp. L735–L738, Dec. 1980.
[11] C. Jacoboni and L. Reggiani, "The Monte Carlo method for the solution of charge transport in semiconductors with applications to covalent materials," *Reviews of Modern Physics*, vol. 55, no. 3, pp. 645–705, 1983.
[12] A. Pacelli, A. W. Duncan, and U. Ravaioli, "A Multiplication Scheme with Variable Weights for Ensemble Monte Carlo Simulation of Hot-Electron Tails," in *Proceedings of IX International Conference on Hot Carriers in Semiconductors*, Chicago, IL, USA,pp. 407–410, July 1995.
[13] V. Sverdlov *et al.*, "Effects of Shear Strain on the Conduction Band in Silicon: An Efficient Two-Band Theory," in *Proceedings of the 37th European Solid-State Device Research Conference (ESSDERC)*, Munich, Germany, pp. 386–389, September 2009.
[14] E. Ungersboeck *et al.*, "The Effect of General Strain on the Band Structure and Electron Mobility of Silicon," *IEEE Transactions on Electron Devices*, vol. 54, no. 9, pp. 2183–2190, 2009.
[15] M. L. Cohen and T. K. Bergstresser, "Band Structures and Pseudopotential Form Factors for Fourteen Semiconductors of the Diamond and Zinc-blende Structures," *Physical Review*, vol. 141, no. 2, pp. 789–796, 2008.
[16] C. Canali *et al.*, "Electron drift velocity in silicon," *Physical Review B*, vol. 12, no. 4, pp. 2265–2284, 2002.

 All Rights Reserved © 2014 IJARCET